Current Research in MRI

Original Article

Diagnostic Efficacy of Multiparametric Magnetic Resonance Imaging Parameters in Differentiating Common Subtypes of Renal Cortical Tumors

İsmet Miraç Çakır[1], Tümay Bekçi[1], Uluhan Eryuruk[1], Nisa Baspinar[2], Serdar Aslan[1]

[1]Department of Radiology, Giresun University, Faculty of Medicine, Giresun, Turkey
[2]Department of Radiology, Cumhuriyet University, Faculty of Medicine, Sivas, Turkey

Cite this article as: Çakır İM, Bekçi T, Eryuruk U, Baspinar N, Aslan S. Diagnostic efficacy of multiparametric magnetic resonance imaging parameters in differentiating common subtypes of renal cortical tumors. *Current Research in MRI*. 2022;1(3):52-58.

Corresponding author: İsmet Miraç Çakır, e-mail: ismetcakir_55@hotmail.com

Received: November 8, 2022 **Accepted:** December 23, 2022

DOI:10.5152/CurrResMRI.2022.221935

Abstract

Objective: The purpose of study was to assess the diagnostic efficacy of multiparametric magnetic resonance imaging in differentiating common subtypes of renal cortical tumors.

Methods: The study group was formed with 85 renal cortical tumors of 75 patients who underwent surgery for renal mass and who had preoperative multiparametric magnetic resonance imaging. Two radiologists were blinded to pathology results evaluated using T2-weighted images, apparent diffusion coefficient maps, and dynamic contrast-enhanced T1-weighted images. T2 signal intensity ratio, apparent diffusion coefficient ratio, corticomedullary phase enhancement ratio, nephrogenic phase enhancement ratio, and delayed phase enhancement ratio were calculated for each tumor type.

Results: Between clear cell renal cell carcinomas and papillary renal cell carcinomas, T2 signal intensity ratio, corticomedullary phase enhancement ratio, nephrogenic phase enhancement ratio, and apparent diffusion coefficient ratio were statistically significantly different ($P < .001$, $P < .001$, $P = .003$, $P = .03$, respectively). Also, there was a significant difference in corticomedullary phase enhancement ratio between clear cell renal cell carcinomas and chromophobe renal cell carcinoma ($P = .031$). Between papillary renal cell carcinomas and chromophobe renal cell carcinomas, T2 signal intensity ratio ($P < .001$), corticomedullary phase enhancement ratio ($P < .001$), nephrogenic phase enhancement ratio ($P = .007$), delayed phase enhancement ratio ($P = .004$), and apparent diffusion coefficient ratio ($P < .001$) were statistically significantly different. Nephrogenic phase enhancement ratio and delayed phase enhancement ratio showed a significant difference between chromophobe renal cell carcinomas and oncoctyomas ($P = .038$ and $P = .032$, respectively). The most efficient parameter in distinguishing clear cell renal cell carcinoma was corticomedullary phase enhancement ratio, and the sensitivity was 80.4% and the specificity was 73.5% with a cutoff value of 283.6.

Conclusion: We think that the use of multiparametric magnetic resonance imaging quantitative parameters was useful in differentiating subtypes of renal cortical tumors.

Keywords: Diffusion-weighted imaging, magnetic resonance imaging, oncocytomas, renal cell carcinomas, renal cortical tumors

INTRODUCTION

Renal cell carcinoma (RCC) is the most frequent renal malignancy in adults and has 3 main subtypes: clear (75%), papillary (10%-15%), and chromophobe (5%) forms.[1,2] Prognosis of papillary and chromophobe subtypes is better than clear cell RCCs.[3] Oncocytomas compose 3%-7% of solid renal tumors and are known to be benign neoplasms. Oncocytomas have similar origin as chromophobe RCCs and therefore have convergent histological and imaging features.[4]

The histopathology of approximately 10%-30% of renal tumors excised surgically is benign.[5,6] In order to avoid unnecessary surgical operations, an image-guided biopsy is recommended before treatment; however, its use remains controversial as it is invasive and not time efficient.[7-9] In elderly or inoperative patients, treatment predilections such as active surveillance and focal ablation are used as an alternative to surgery in clinical practice. The presence of less invasive alternative treatment methods has led to a clinical need for accurate recognition of renal lesions before treatment to avoid potentially inadequate treatment.[10] Multiparametric magnetic resonance imaging (mpMRI) established on various anatomic and functional parameters have an important role and add diagnostic value in the detection and differentiation of renal cortical tumors.[11] Magnetic resonance imaging may be beneficial in distinguishing benign solid renal masses from some RCC subtypes and foreseeing the histologic grade of a tumor and play a crucial role in ensuring appropriate patient management to avoid unnecessary surgery or other interventions.

The purpose of this study was to assess the diagnostic efficacy of mpMRI differentiating frequent subtypes of renal cortical tumors.

METHODS

Patient Group

This single-institution, retrospective study was approved by the institutional ethics committee, and informed consent was waived (ethics committee number: 11484, date: September 25, 2022). In our study, the hospital database images of patients older than 18 years who had partial or radical nephrectomy surgery because of malignant renal masses between May 2018 and January 2022 were scanned retrospectively. Preoperative abdominal MRIs were performed in 98 of the patients. As the pathology results of 8 of the 98 patients could not be accessed, and the MRI examination of 5 patients was carried out without a contrast agent, these patients were excluded from the study. Three patients with histopathological results compatible with angiomyolipoma (AML) and 7 patients with rare forms of RCCs (multilocular, cystic carcinoma, tubulocystic renal cell carcinoma, and papillary adenoma) were excluded. Seventy-five patients overall with 85 renal cortical tumors were included in the study, with 1 patient having bilateral and 5 patients having multifocal renal cortical tumors. Fifty-one of tumors were reported as clear cell carcinoma, 16 were reported as papillary cell carcinoma, 8 were reported as chromophobe cell carcinoma, and 10 as oncocytoma. The study flow chart is shown in Figure 1.

MAIN POINTS

- Multiparametric magnetic resonance imaging plays a crucial role and adds diagnostic value in the detection and differentiation of the renal cortical tumors.
- Corticomedullary phase enhancement ratio is the most effective parameter in distinguishing clear cell renal cell carcinomas with an accuracy of 77.7%.
- Multiparametric magnetic resonance imaging can be used to recognize non-clear cell renal cell carcinomas in patients at high medical risk for interventional procedures or surgery and to encourage active surveillance in appropriate patients.

Magnetic Resonance Imaging Protocol

All MRI examinations were carried out on the same 1.5-T MRI system (Magnetom Symphony; Siemens Medical Solutions, Erlangen, Germany) with a phased-array body coil. The MRI protocol comprised of the following sequences: turbo-spin echo T2-weighted images (T2WI); axial T2WI with fat suppression (FS); axial gradient-echo T1-weighted images (T1WI) with and without FS; axial diffusion-weighted images (DWIs) with *b*-values of 0, 400, and 800 s/mm^2. Three-dimensional axial T1WI images with FS were obtained both before and after contrast agent. Gadopentetate dimeglumine (Gadovist, Bayer Healthcare, Berlin, Germany) was administered at a dose of 0.1 mL/kg with an injection rate of 3 mL/s, followed by a 10 mL of normal saline infusion. After intravenous gadolinium injection, dynamic contrast enhanced (DCE) images were performed in 3 post-contrast phases, each with a delay of 30 s.

Magnetic Resonance Imaging Evaluation

Magnetic resonance images of 85 renal masses included in the study were estimated retrospectively by 2 radiologists (reader 1 with 11 years of abdominal radiology practice and reader 2 with 10 years), independently of histopathological results. All MRI images were uploaded to a picture archiving communication system. While evaluating T2WI, apparent diffusion coefficient (ADC) maps, and DCE–T1WI, a circular region of interest (ROI) was placed in the tumor and normal cortex parenchyma. The mean ROI size used was 100 mm^2.

T2 measurements were evaluated from both the tumor and non-tumor normal renal cortex. Region of interest measurements were taken from

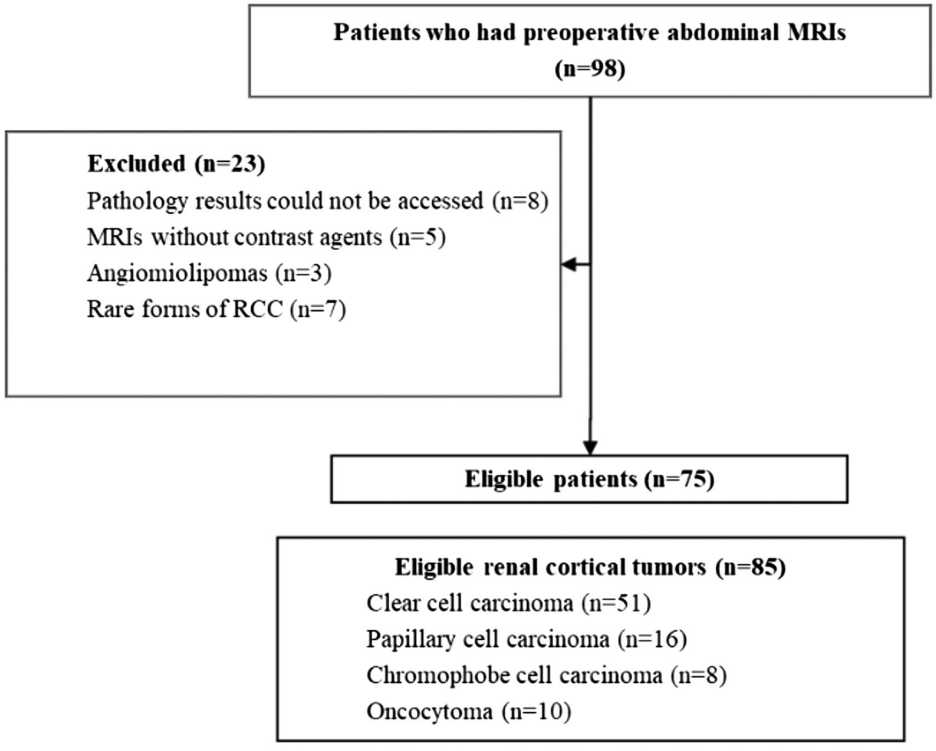

Figure 1. Study flowchart. MRI, magnetic resonance imaging; RCC, renal cell carcinoma.

3 different points in the solid areas of the tumor without necrosis, and the mean value of these measurements was recorded. This measurement was also carried out similar to the normal non-tumor renal cortical area. T2 signal intensity ratio (T2SIR) (tumor (Tu) SI/normal renal cortex (C) SI) × 100 was calculated from the measurements taken from the tumor and normal renal cortex.

In the DCE images, a single ROI was placed over the solid enhancing region without necrosis avoiding vascular structures, cystic components of the tumor, and retroperitoneal adipose tissue in the corticomedullary phase. The tumor enhancement ratio (ER) was calculated from the corticomedullary, nephrogenic, and excretory phases. The ER was calculated as [(post-contrast SI – pre-contrast SI)/pre-contrast SI] × 100. Three ERs were calculated based on the post-contrast phase: an ERc using corticomedullary phase, an ERn using the nephrogenic phase, and an ERd using the delayed phase.

Apparent diffusion coefficient measurements were taken from both the tumor and non-tumor normal renal cortex. Considering T2W and DCE images, ROI measurements were taken from 3 different points in the solid areas of the tumor without necrosis, and the mean value of these measurements was recorded. This measurement was also carried out similar to the normal non-tumor renal cortical area. The ADC ratio (ADCr) (tumor ADC/normal renal cortex ADC) × 100 was calculated from the measurements taken from the tumor and normal renal cortex.

All quantitative parameters were calculated independently by 2 readers. Disputes among readers were resolved by consulting a radiologist with 12 years of abdominal radiology experience.

Statistical Analysis

IBM Statistical Package for Social Sciences version 25.0 (IBM SPSS Corp.; Armonk, NY, USA) statistical analysis software was used in the analysis of the data. Shapiro–Wilk test was used to evaluate the normality of quantitative data distribution. The Mann–Whitney *U* test and Kruskal–Wallis test were used to compare quantitative data that did not exhibit normal distribution. The Bonferroni correction was carried out for the comparison of more than 2 groups. A receiver operating characteristic analysis was used to determine the cutoff values of radiological parameters for the prediction of the pathologically diagnosed clear cell RCC. Therefore, the area under the curve, sensitivity, and specificity values were calculated. Data were presented as mean ± SD and n (%). *P* values of <.05 were considered statistically significant.

Table 1. Quantitative Parameters for Common Renal Cortical Tumor Types

	Clear Cell RCC	Papillary RCC	Chromophobe RCC	Oncocytoma
T2SIR				
R1	129.3 ± 34.7	84.2 ± 17.3	121.2 ± 11.7	140.7 ± 36.1
R2	133.5 ± 44.2	95.3 ± 26.3	114.4 ± 10.2	174.2 ± 44.2
ERc				
R1	332.5 ± 62.2	182.3 ± 38.5	248.6 ± 52.1	319.3 ± 47.9
R2	310.2 ± 48.2	188.1 ± 42.2	233.5 ± 49.4	308.4 ± 42.5
ERn				
R1	316.9 ± 63.9	247.7 ± 56.9	244.4 ± 50.1	360.7 ± 103.1
R2	322.4 ± 72.4	259.5 ± 61.3	249.5 ± 53.4	369.1 ± 112.3
ERd				
R1	302.8 ± 67.1	260.9 ± 46.6	241.2 ± 49.4	371.6 ± 125.8
R2	314.8 ± 71.7	271.3 ± 55.9	249.6 ± 55.2	383.2 ± 133.4
ADCr				
R1	92.4 ± 15.9	60.4 ± 21.4	85.5 ± 12.8	108 ± 27.6
R2	96.3 ± 17.2	58.4 ± 19.2	89.6 ± 13.4	101 ± 26.7

ADCr, apparent diffusion coefficient ratio; ERc, corticomedullary phase enhancement ratio; ERd, delayed phase enhancement ratio; ERn, nephrogenic phase enhancement ratio; R1, reader 1; R2, reader 2; RCC, renal cell carcinoma; T2SIR, T2 signal intensity ratio.

RESULTS

Patient Demographics and Renal Tumors

The mean age of the patients was 56.7 ± 11.5 years (range: 18-85). Thirty-three (38.8%) of the patients were female and 52 (61.2%) were male. The mean tumor size was 45.6 mm (median: 40, range: 8-127) for clear cell RCCs, 36.5 mm (median: 29.5, range: 11-98) for papillary RCCs, 62.8 mm (median: 76, range: 18-114) for chromophobe RCCs,

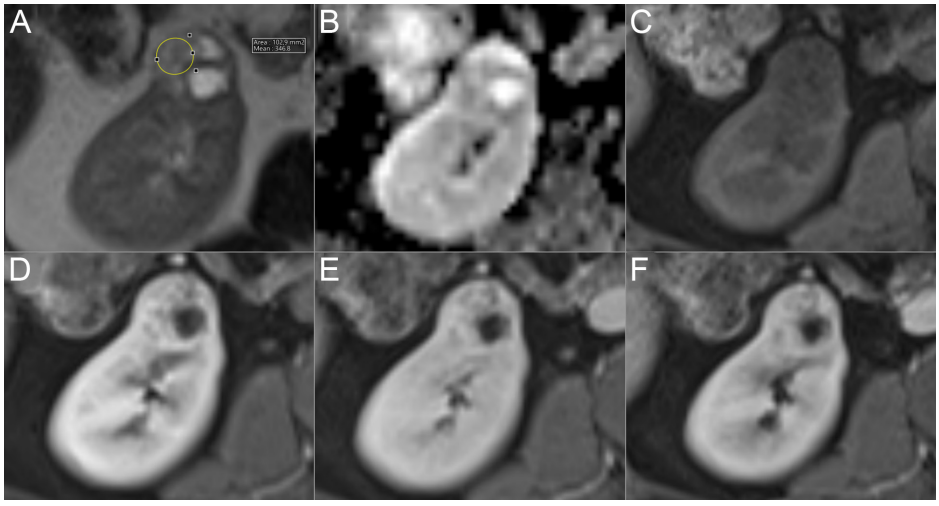

Figure 2. Clear cell renal cell carcinoma in the right kidney of a 63-year-old man. (A) Axial T2-weighted magnetic resonance (MR) image shows the renal mass with high signal intensity compared with renal parenchyma (T2SIR = 109.3). A region of interest has been drawn in the solid enhancing region without necrosis avoiding vascular structures and cystic components of the tumor and then reported on all sequences. (B) Apparent diffusion coefficient (ADC) maps show slight restriction of diffusion in the renal mass (ADCr = 83.6). Axial non-enhanced (C) and contrast-enhanced T1-weighted MR images in corticomedullary (D), nephrogenic (E), and delayed (F) phases show early and intense enhancement of mass in corticomedullary phase followed by washout (ERc: 366.6 , ERn: 329.5, ERd: 321.1). ADCr, ADC ratio; ERc, corticomedullary phase enhancement ratio; ERd, delayed phase enhancement ratio; ERn, nephrogenic phase enhancement ratio.

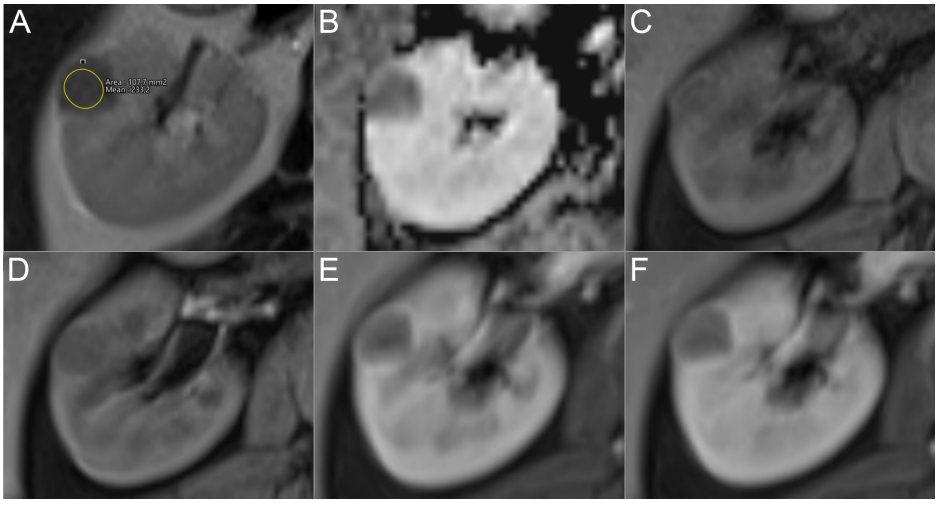

Figure 3. Papillary renal cell carcinoma in the right kidney of a 51-year-old man. (**A**) Axial T2-weighted magnetic resonance (MR) image shows significant a renal mass with low signal intensity compared to renal parenchyma (T2SIR = 67). (B) Apparent diffusion coefficient (ADC) maps show markedly low ADC values in the renal mass (ADCr = 44.5). Axial non-enhanced (C) and contrast-enhanced T1-weighted MR images in corticomedullary (D), nephrogenic (E), and delayed (F) phases show slowly increasing enhancement of the mass (ERc: 78.2, ERn: 93.4, ERd: 121.7). ADCr, ADC ratio; ERc, corticomedullary phase enhancement ratio; ERd, delayed phase enhancement ratio; ERn, nephrogenic phase enhancement ratio.

and 33.8 mm (median: 29, range: 18-87) for oncocytomas. There were statistically significant differences in tumor sizes between chromophobe RCCs and papillary RCCs and between chromophobe RCCs and oncocytoma ($P < .012$). No significant difference in size was observed between other tumor groups.

Multiparametric Magnetic Resonance Imaging the Quantitative Analysis of Renal Tumors

Table 1 presents the results of 2 readers for all the evaluated MRI parameters.

Interobserver agreement was almost perfect, with weighted K values ranging from 0.89 to 0.93 in the calculation of MRI quantitative parameters.

There was a statistically significant difference between papillary RCCs and the other renal cortical tumors in T2SIR ($P < .001$).

Considering the post-contrast dynamic behavior, there was a statistically significant difference between clear cell RCCs (Figure 2) and papillary RCCs (Figure 3), clear cell RCCs and chromophobe RCC (Figure 4), and papillary RCC and oncocytoma (Figure 5) in ERc ($P < .001$, $P = .031$ and $P < .001$, respectively). There was a statistically significant difference between clear cell RCC and papillary RCC, chromophobe RCC and oncocytoma, and papillary RCC and oncocytoma in ERn ($P = .004$, $P = .038$ and $P = .007$, respectively). There was a statistically significant difference between chromophobe RCC and oncocytoma and between papillary RCC and oncocytoma in ERd ($P = .040$ and $P = .031$, respectively) (Table 2).

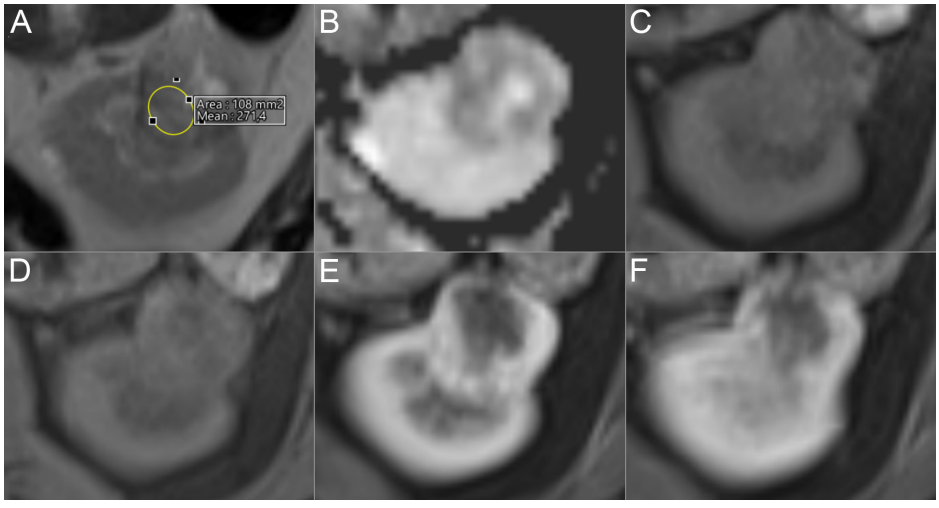

Figure 4. Chromophobe renal cell carcinoma in the left kidney of a 39-year-old man. (A) Axial T2-weighted magnetic resonance (MR) image shows a renal mass with almost the same signal intensity compared to renal parenchyma (T2SIR = 98). (B). Apparent diffusion coefficient (ADC) maps show diffusion restriction in the solid areas of renal mass (ADCr = 59.5). Axial non-enhanced (C) and contrast-enhanced T1-weighted MR images in corticomedullary (D), nephrogenic (E), and delayed (F) phases show moderate enhancement of the mass without washout (ERc: 122.6, ERn: 126.6, ERd: 128). ADCr, ADC ratio; ERc, corticomedullary phase enhancement ratio; ERd, delayed phase enhancement ratio; ERn, nephrogenic phase enhancement ratio.

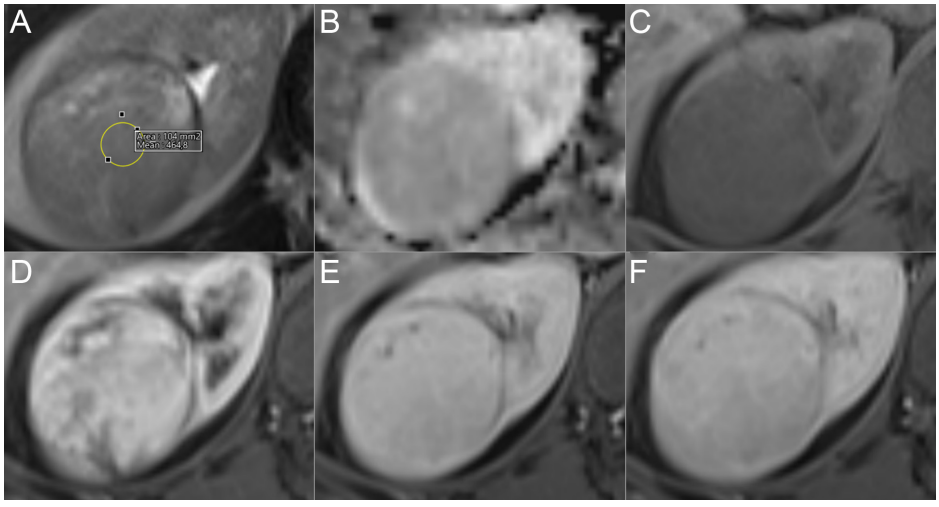

Figure 5. Oncocytoma in the right kidney of a 41-year-old man. (A) Axial T2-weighted magnetic resonance image shows a renal mass with slightly high SI compared to renal parenchyma (T2SIR = 116). (B) Apparent diffusion coefficient (ADC) maps show diffusion restriction in the renal mass (ADCr = 75). Axial non-enhanced (C) and contrast-enhanced T1-weighted MR images in corticomedullary (D), nephrogenic (E), and delayed (F) phases show strong heterogenous enhancement of mass in corticomedullary followed by washout (ERc: 281.9, ERn: 259, ERd: 250.4). ADCr, ADC ratio; ERc, corticomedullary phase enhancement ratio; ERd, delayed phase enhancement ratio; ERn, nephrogenic phase enhancement ratio.

There was a statistically significant difference in ADCr between clear cell RCC and papillary RCC, and between papillary RCC and oncocytoma ($P < .001$).

Recognition of Clear Cell Renal Cell Carcinoma

The most efficient parameters in discriminating clear cell RCC from other renal cortical tumors were ERc and T2SIR (Table 3). Between the 2 tumor groups, sensitivity was 80.4% and specificity was 73.5% in ERc with a cutoff value of 283.6 and sensitivity was 78.4% and specificity 70.6% in T2SIR with a cutoff value of 107.2 (Figure 6).

DISCUSSION

In our study, T2 signal ratios, ADCr, and ER parameters obtained from mpMRI examination had high diagnostic accuracy in differentiating common subtypes of renal cortical tumors.

Each subtype of renal cortical tumors has different T2 signal properties as they have different histological, morphological, and genetic characteristics. Clear cell RCCs tend to be hyperintense on T2WI due to necrosis and/or cystic degeneration. Papillary cell RCCs are usually hypointense on T2WI due to hemosiderin deposition.[12,13] Whereas, chromophobe RCCs tend to have moderate-to-low T2 signals. T2 signals of oncocytomas are usually high compared to the renal cortex,

Table 2. Statistically Significant *P* Values of the Quantitative Characteristics Between Each Renal Cortical Tumor Type

	Clear Cell RCC and Papillary RCC	Clear cell RCC and Chromophobe RCC	Clear cell RCC and Oncocytoma	Papillary RCC and Chromophobe RCC	Papillary RCC and Oncocytoma	Chromophobe RCC and Oncocytoma
T2SIR	**<.001**	1.000	1.000	**<.001**	**<.001**	1.000
ERc	**<.001**	**.031**	1.000	.639	**<.001**	.352
ERn	**.004**	.075	1.000	1.000	**.007**	**.038**
ERd	.264	.202	.813	1.000	**.040**	**.031**
ADCr	**.001**	1.000	1.000	.317	**<.001**	.424

ADCr, apparent diffusion coefficient ratio; ERc, corticomedullary phase enhancement ratio; ERd, delayed phase enhancement ratio; ERn, nephrogenic phase enhancement ratio; RCC, renal cell carcinoma; T2SIR, T2 signal intensity ratio. Statistically significant p values are in bold format.

Table 3. Results of ROC Analysis and Measures of Accuracy in Determining Clear Cell RCC

	T2SIR	ERc	ERn	ERe	ADCr
AUC	0.771 (0.662-0.881)	0.828 (0.736-0.921)	0.668 (0.543-0.793)	0.59 (0.463-0.717)	0.682 (0.55-0.814)
P	<.001	<.001	.009	.162	.005
Cutoff	107.2	283.6	291.1	283.05	80.25
Sensitivity	78.4 (64.68-88.71)	80.4 (66.88-90.18)	74.5 (60.37-85.67)	54.9 (40.34-68.87)	84.3 (71.41-92.98)
Specificity	70.6 (52.52-84.9)	73.5 (55.64-87.12)	61.8 (43.56-77.83)	52.9 (35.13-70.22)	58.8 (40.7-75.35)
PPV	80 (69.97-87.29)	82 (71.91-89.02)	74.5 (64.94-82.19)	63.6 (53.12-72.99)	75.4 (66.89-82.36)
NPV	68.6 (55.32-79.36)	71.4 (58.06-81.87)	61.8 (48.52-73.46)	43.9 (33.55-54.82)	71.4 (55.49-83.37)
Accuracy	75.3 (64.75-84.01)	77.7 (67.31-85.97)	69.4 (58.47-78.95)	54.1 (42.96-64.98)	74.1 (63.48-83.02)

ADCr, apparent diffusion coefficient ratio; AUC, area under curve; ERc, corticomedullary phase enhancement ratio; ERd, delayed phase enhancement ratio; ERn, nephrogenic phase enhancement ratio; NPV, negative predictive value; PPV, positive predictive value; RCC, renal cell carcinoma; T2SIR, T2 signal intensity ratio.

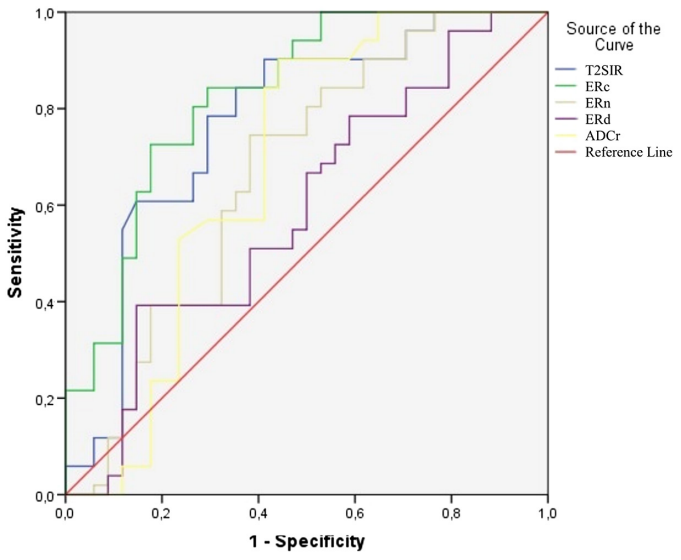

Figure 6. Receiver operating characteristic curves for parameters T2 signal intensity ratio (T2SIR), corticomedullary phase enhancement ratio (ERc), nephrogenic phase enhancement ratio (ERn), delayed phase enhancement ratio (ERd), and apparent diffusion coefficient ratio (ADCr).

and a hypointense stellate scar may be found in the central part.[14] In a study, Cornelis et al[15] determined that the T2 signal ratio was the lowest in papillary RCCs and AMLs of renal cortical tumors, while this rate was higher in chromophobe RCCs, clear cell RCCs, and oncocytomas. In our work, parallel to the literature, T2SIR was the lowest in papillary RCCs, and there was a statistically significant difference in the differentiation from other types of tumors. In the univariate analysis, T2SIR was statistically different in distinguishing between clear cell RCCs and other renal cortical tumors ($P = .004$). Between the 2 tumor groups, sensitivity was 78.4% and specificity was 70.6% in T2SIR with a cutoff value of 107.2. The use of TSIR in multiparametric MRI plays a crucial role in the differentiation of subtypes of renal cortical tumors by increasing the diagnostic efficiency.

Diffusion-weighted imaging, which provides information on the cell density, has been valuable in oncological imaging and has also been used for differentiation of RCC subtypes. Most researchers briefed that the ADC values of clear cell RCCs are higher compared to RCC subtypes but are similar to oncocytomas.[16,17] As ADC values vary based on devices and magnetic field strength, we used the ADCr in our study, which we considered could eliminate these differences. There are few studies in the literature that differentiate RCCs using the ADCr.[15,18,19] Zhong et al[18] used ADCr to distinguish oncocytoma from chromophobe RCCs and found a statistically significant difference. In our study, the highest ADCr was in oncocytoma and the lowest ADCr was in papillary RCCs. There was a statistically significant difference between papillary RCCs and oncocytoma and between papillary RCC and clear cell RCC ($P < .001$). The findings of our study were parallel to those of the study by Cornelius et al.[15] In differentiating clear cell RCC and other renal cortical tumors, the sensitivity was 84.3 and the specificity was 58.8, with a cutoff value of 0.80 in ADCr. We think that this may be employed as a determining parameter in the differentiation of RCC subtypes, regardless of the device.

As clear cell RCC is known to have higher vascularity than other RCC subtypes, such as chromophobe RCCs and especially papillary RCCs, researchers have aimed to differentiate renal tumor subtypes based on the degree of enhancement of tumors on contrast enhanced computerized tomography and MRIs.[20-23] These researchers identified statistically significant differences between the degree of enhancement in different RCC subtypes. Also, this made it difficult to distinguish clear cell RCC with contrast-enhancement alone, as the contrast levels of clear cell RCC and other renal cortical tumors, especially oncocytoma and angiomyolipoma, were generally similar.[24] In our work, there was a statistically significant difference between papillary RCC and both clear cell RCC and oncocytoma in ERc and ERn ($P < .008$). There was a statistically significant difference between chromophobe RCCs and clear cell RCCs in ERc and between chromophobe RCCs and oncocytoma in ERn and ERd ($P = .031$, $P = .038$ and $P = .031$, respectively). In the logistic regression analysis between clear cell RCC and other renal cortical tumors, the parameters that were statistically significant in both univariate and multivariate analyses were ERc and ERn ($P < .001$). The most effective parameter in the differentiation of the 2 groups was ERc, with a cutoff value of 283.6; sensitivity was 80.4%, specificity was 73.5%, positive predictive value was 82%, negative predictive value was 71.4%, and accuracy was 77.7%. Multiparametric magnetic resonance imaging can be used to distinguish clear cell RCC from other renal cortical tumors in patients with small tumors that are less likely to be diagnosed by biopsy or who are at high medical risk for interventional procedures.

Our study has some limitations. First, it is designed retrospectively. While readers are blinded to the final pathology, there is inherent bias in this structure. Second, ROI locations and assessments were made in agreement with 2 radiologists, and interobserver variability was not calculated. Studies with more than 1 reader will confirm these results. Third, the number of chromophobe RCCs in our study was low in proportion to the incidence of this subtype among society. At last, our study did not cover the entire RCC spectrum, as undifferentiated RCC subtypes and other rarer subtypes were not included in our study. However, we do not think these 3 subtypes we selected affect the power of our study as they constitute 90% of all RCCs encountered in clinical practices.

CONCLUSION

We think that the diagnostic sensitivity and specificity of mpMRI, including T2SIR and ERc, which is used to distinguish clear cell RCC from other common subtypes of renal cortical tumors, is high. The use of the quantitative parameters of mpMRI may be useful in treatment planning in elderly patients with comorbidities at high risk for biopsy or surgery, or to encourage active surveillance where appropriate.

Ethics Committee Approval: Ethics committee approval was received for this study from the ethics committee of Kanuni Training and Research Hospital Institutional Review Board (Date: September 25, 2022, Decision No: 11484) .

Informed Consent: Retrospective study was approved by the institutional ethics committee, and informed consent was waived.

Peer-review: Externally peer-reviewed.

Author Contributions: Concept – IM.C., U.E.; Design – IM.C., T.B.; Supervision – S.A., N.B.; Materials – IM.C., N.B.; Data Collection and/or Processing – IM.C., U.E.; Analysis and/or Interpretation – T.B, S.A.; Literature Review – IM.C., T.B.; Writing – IM.C., U.E.; Critical Review – U.E., S.A.

Declaration of Interests: The authors declare that they have no conflicts ofinterest.

Funding: The authors declare that this study has received no financial support.

REFERENCES

1. Muglia VF, Prando A. Renal cell carcinoma: histological classification and correlation with imaging findings. *Radiol Bras*. 2015;48(3):166-174. [CrossRef]
2. Manley BJ, Hsieh JJ. Sarcomatoid renal cell carcinoma: genomic insights from sequencing of matched sarcomatous and carcinomatous components. *Transl Cancer Res*. 2016;5(suppl 2):S160-S165. [CrossRef]
3. Deng J, Li L, Xia H, et al. A comparison of the prognosis of papillary and clear cell renal cell carcinoma: evidence from a meta-analysis. *Med (Baltim)*. 2019;98(27):e16309. [CrossRef]
4. Wobker SE, Williamson SR. Modern pathologic diagnosis of renal oncocytoma. *J Kidney Cancer VHL*. 2017;4(4):1-12. [CrossRef]
5. Sanchez A, Feldman AS, Hakimi AA. Current management of small renal masses, including patient selection, Renal Tumor Biopsy, Active Surveillance, and Thermal Ablation. *J Clin Oncol*. 2018;36(36):3591-3600. [CrossRef]
6. Leone AR, Diorio GJ, Spiess PE, Gilbert SM. Contemporary issues surrounding small renal masses: evaluation, diagnostic biopsy, nephron sparing, and novel treatment modalities. *Oncology (Williston Park)*. 2016;30(6):507-514.
7. Pagnini F, Cervi E, Maestroni U, et al. Imaging guided percutaneous renal biopsy: do it or not? *Acta Biomed*. 2020;91(8-S):81-88. [CrossRef]
8. Brachemi S, Bollée G. Renal biopsy practice: what is the gold standard? *World J Nephrol*. 2014;3(4):287-294. [CrossRef]
9. Hogan JJ, Mocanu M, Berns JS. The native kidney biopsy: update and evidence for best practice. *Clin J Am Soc Nephrol*. 2016;11(2):354-362. [CrossRef]
10. Hötker AM, Mazaheri Y, Wibmer A, et al. Differentiation of clear cell renal cell carcinoma from other renal cortical tumors by use of a quantitative multiparametric MRI approach. *AJR Am J Roentgenol*. 2017;208(3):W85-W91. [CrossRef]
11. Diaz de Leon A, Costa D, Pedrosa I. Role of multiparametric MR imaging in malignancies of the urogenital tract. *Magn Reson Imaging Clin N Am*. 2016;24(1):187-204. [CrossRef]
12. Lu D, Yuan W, Zhu Q, Ye J, Zhu W, Chen W. Comparative study of CT and MRI appearances in mucinous tubular and spindle cell carcinoma and papillary renal cell carcinoma. *Br J Radiol*. 2021;94(1126):20210548. [CrossRef]
13. Wang ZJ, Zagoria RJ. Invited commentary on "differentiation of solid renal tumors with multiparametric MR imaging". *RadioGraphics*. 2017;37(7):2042-2044. [CrossRef]
14. Lopes Vendrami C, Parada Villavicencio C, Dejulio TJ, et al. Differentiation of solid renal tumors with multiparametric MR imaging. *RadioGraphics*. 2017;37(7):2026-2042. [CrossRef]
15. Cornelis F, Tricaud E, Lasserre AS, et al. Routinely performed multiparametric magnetic resonance imaging helps to differentiate common subtypes of renal tumours. *Eur Radiol*. 2014;24(5):1068-1080. [CrossRef]
16. Wang H, Cheng L, Zhang X, et al. Renal cell carcinoma: diffusion-weighted MR imaging for subtype differentiation at 3.0 T. *Radiology*. 2010;257(1):135-143. [CrossRef]
17. Cova M, Squillaci E, Stacul F, et al. Diffusion-weighted MRI in the evaluation of renal lesions: preliminary results. *Br J Radiol*. 2004;77(922):851-857. [CrossRef]
18. Zhong Y, Wang H, Shen Y, et al. Diffusion-weighted imaging versus contrast-enhanced MR imaging for the differentiation of renal oncocytomas and chromophobe renal cell carcinomas. *Eur Radiol*. 2017; 27(12):4913-4922. [CrossRef]
19. Ludwig DR, Ballard DH, Shetty AS, Siegel CL, Yano M. Apparent diffusion coefficient distinguishes malignancy in T1-hyperintense small renal masses. *AJR Am J Roentgenol*. 2020;214(1):114-121. [CrossRef]
20. Young JR, Margolis D, Sauk S, Pantuck AJ, Sayre J, Raman SS. Clear cell renal cell carcinoma: discrimination from other renal cell carcinoma subtypes and oncocytoma at multiphasic multidetector CT. *Radiology*. 2013;267(2):444-453. [CrossRef]
21. Vargas HA, Chaim J, Lefkowitz RA, et al. Renal cortical tumors: use of multiphasic contrast-enhanced MR imaging to differentiate benign and malignant histologic subtypes. *Radiology*. 2012;264(3):779-788. [CrossRef]
22. Kim JH, Bae JH, Lee KW, Kim ME, Park SJ, Park JY. Predicting the histology of small renal masses using preoperative dynamic contrast-enhanced magnetic resonance imaging. *Urology*. 2012;80(4):872-876. [CrossRef]
23. Sun MR, Ngo L, Genega EM, et al. Renal cell carcinoma: dynamic contrast-enhanced MR imaging for differentiation of tumor subtypes--correlation with pathologic findings. *Radiology*. 2009;250(3):793-802. [CrossRef]
24. Pierorazio PM, Hyams ES, Tsai S, et al. Multiphasic enhancement patterns of small renal masses (≤4 cm) on preoperative computed tomography: utility for distinguishing subtypes of renal cell carcinoma, angiomyolipoma, and oncocytoma. *Urology*. 2013;81(6):1265-1271. [CrossRef]